Available online at www.sciencedirect.com
SCIENCE DIRECT®
Journal of Sound and Vibration 291 (2006) 258–274
JOURNAL OF SOUND AND VIBRATION
www.elsevier.com/locate/jsvi

A switched stiffness approach for structural vibration control: theory and real-time implementation

Arun Ramaratnam, Nader Jalili*

Smart Structures and Nanoelectromechanical Systems Laboratory, Department of Mechanical Engineering, Clemson University, Clemson, South Carolina 29634-0921, USA

Received 15 June 2004; received in revised form 6 May 2005; accepted 7 June 2005
Available online 24 August 2005

Abstract

A simple semi-active structural vibration control based on switching the system equivalent stiffness between two distinct values is proposed. When the system is moving away from its equilibrium state, the stiffness of the system is set to the higher value, and when it returns to its equilibrium, it is set to the lower value. Termed here "switched stiffness", this vibration control method leads to change in the stored potential energy, which results in reduced total energy of the system. The switched stiffness can be typically implemented using a bi-stiffness spring setting, with the resulting relay-type control logic based on the position and velocity feedback. Unavailability of velocity sensors makes it difficult to implement this simple control logic. Although, numerical differentiation of the position signal can be utilized to acquire the velocity, but intervention of noise and the resulting signal phase-lag due to the filters used may degrade the vibration suppression performance. Hence, a novel output feedback variable structure observer, robust in nature, is used to estimate the required velocity signal. A single degree of freedom setup is considered to experimentally implement the switched stiffness concept proposed here. Simulations and experimental results demonstrate the effectiveness of the vibration suppression method proposed here.

*Corresponding author. Tel.: +1 864 656 5642; fax: +1 864 656 4435.
E-mail address: jalili@clemson.edu (N. Jalili).
URL: http://www.ces.clemson.edu/ssnems.

0022-460X/$ - see front matter © 2005 Elsevier Ltd. All rights reserved.
doi:10.1016/j.jsv.2005.06.012

1. Introduction

Active vibration control concepts are best suited for suppressing the structural vibrations of dynamic systems. However, their energy inputs are typically high and may lead to system instability under certain conditions. Intervention of noise and the phase lag, introduced by filters used to remove the ever-present noise, have also been notorious problems that are faced frequently in the domain of vibration control. Even a robust active control could lead to instability because of the phase lag produced by noise filters [1]. Passive vibration control methods, on the other hand, are less effective in vibration control with slower response time, but are relatively simpler and have much more improved stability characteristics compared to active systems [2]. There is always a trade-off between active and passive vibration control methods, which has led to the development of hybrid methods such as adaptive passive and semi-active configurations [3,4].

A recent development in the area of vibration control utilizes the concept of switched stiffness [5–8]. The switched stiffness method is a semi-active vibration control method, where the energy of the system is dissipated by changing the values of the spring stiffness. A simple control law, based on the position and velocity feedback, is designed to switch the stiffness of the spring in order to increase the energy dissipation from the system. The spring should possess two distinct stiffness values, referred to as high stiffness (for the higher value) and low stiffness (for the lower value). The high stiffness state is used when the system is moving away from its equilibrium such that the potential energy stored in the system is maximized. The spring is switched to low stiffness state when the system has reached its maximum stored potential energy, which occurs when the system has attained its maximum amplitude of vibration for that halfcycle. Thus, the stiffness switching results in the loss of some of the potential energy. The energy is dissipated in the system by this loss of potential energy. The reduced potential energy is then converted to kinetic energy, that is lower than the kinetic energy during the previous cycle due to the lost energy by changing the spring stiffness.

This energy dissipation method can be used for vibration suppression of transient and continuously excited systems. However, limitations for implementation of this type of vibration attenuation are the velocity measurement requirement of the system under study and availability of a bi-stiffness spring configuration in practice. Expensive velocity sensors and noisy differentiators make the first limitation even more noticeable. This problem can be overcome by implementing an output feedback velocity observer developed by Xian et al. [9]. A bi-stiffness spring may be designed, but to the best knowledge of the authors such commercial setup do not exist in practice.

In this paper, a switched stiffness control strategy is proposed for vibration suppression of mechanical systems. Past research in vibration control using variable stiffness also prove that such concept to be effective [10–13]. A single degree-of-freedom (sdof) system is considered here to demonstrate the concept. Numerical simulations are performed to analyze the behavior of the system. Experimental validation of the concept using a rectilinear plant is also presented to verify the numerical results. The experimental setup consists of an excitation source and a mass–spring system. The spring is modified using an external element and a motor to take up two stiffness values according to the control law. The control objective here is to suppress the vibration transients in the system in the presence of the excitation and disturbances. The controller

developed here is a semi-active controller utilizing stiffness switching concept. The position of the system is fed back using an encoder, while the velocity of the system is estimated using an output feedback variable structure observer [9]. The results obtained by switching the stiffness demonstrate that the system residual vibrations can be suppressed effectively.

The concept of switched systems can be easily implemented using piezoelectric materials, as these materials possess the ability to change their equivalent effective stiffness according to the type of circuit connection [5–8,14]. More specifically, when connected in an open circuit, the piezoelectric material exhibits a particular stiffness and when short-circuited, it exhibits different value, typically lower stiffness. This ability of the piezoelectric materials to change their stiffness is due to their ability to change their mechanical compliance, caused by changes in their electrical impedance when connected in open or short circuit [6].

The rest of the paper is organized as follows. In the immediately following section, the switched stiffness vibration control concept is explained along with the control law and stability analysis. Section 3 discusses real-time implementation of the switched stiffness concept using velocity observer, followed by a modified velocity observer derivations. Numerical results are provided in Section 4, with the experimental results and discussions given in Section 5. Section 6 summarizes the paper and provides future directions.

2. Switched stiffness vibration control concept

Switched stiffness vibration control method can be best explained by taking a sdof mass–spring system as shown in Fig. 1. The governing equation is simply given by

$$m\ddot{y}(t) + k(t)y(t) = f(t), \tag{1}$$

where $y(t)$ is the system output (i.e., the signal that is to be attenuated), m is the mass, $k(t)$ is the stiffness and $f(t)$ is the external force acting on the system. The spring is assumed to possess a step-variable stiffness setting in the sense that it can be switched between two distinct values, namely high and low stiffness values. As the external force $f(t)$ causes the mass to move away from its equilibrium position, the stiffness of the spring $k(t)$ is kept at the high value. The maximum potential energy at maximum mass displacement is simply $\frac{1}{2}k_{\text{high}}y_{\max}^2$. At this point

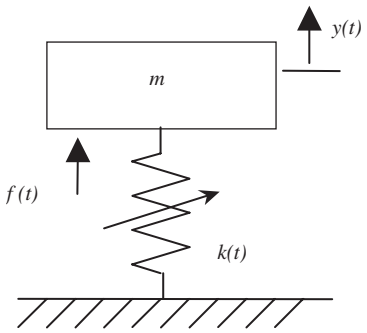

Fig. 1. The sdof mass–spring system with variable stiffness.

(y_{max}), the stiffness is switched to low value and kept at this value until the mass reaches the equilibrium point again. Therefore, the potential energy at y_{max} becomes $\frac{1}{2}k_{low}y_{max}^2$. The loss in potential energy can be given as $\frac{1}{2}\Delta k y_{max}^2$, where $\Delta k = k_{high} - k_{low}$.

The decrease in potential energy given by $\frac{1}{2}\Delta k y_{max}^2$ will consequently result in decrease in converted kinetic energy, thereby introducing energy dissipation in the system. The stiffness is then switched back to the high value when the system moves away from its equilibrium, thus switching stiffness from low to high in a periodic manner to gradually dissipate system energy. The sdof system is no more conservative due to the dependence of the stiffness with time. Hence, the system becomes a parametric system (with quasi time-varying parameters) and the work done by such non-conservative spring force is the means of energy dissipation [15].

2.1. Control law for switching stiffness

A heuristic control law was suggested to essentially switch the stiffness values through a hard switching or on–off (relay) control [5]. The control law is based on the position of the system with respect to the equilibrium state. The control law can be stated as

$$\begin{aligned} k(t) &= k_{high} \quad \text{for } y\dot{y} \geqslant 0, \\ k(t) &= k_{low} \quad \text{for } \dot{y}y < 0. \end{aligned} \tag{2}$$

The control law can also be expressed in the following more compact form:

$$k(t) = \frac{(k_{high} + k_{low})}{2} + \frac{(k_{high} - k_{low})\text{sgn}(y\dot{y})}{2} \quad \text{for } k_{low} \leqslant k \leqslant k_{high}. \tag{3}$$

Defining, $\bar{K}_1 = (k_{high} + k_{low})/2$ and $\bar{K}_2 = (k_{high} - k_{low})/2$, it yields

$$k(t) = \bar{K}_1 + \bar{K}_2\ \text{sgn}(y\dot{y}). \tag{4}$$

For numerical simulations, the spring stiffness value is changed such that the potential energy is dissipated at maximum deflection, resulting in the "step-down" of total system energy, and hence, suppressing the displacement as shown in Fig. 2. The amount of dissipated energy over a particular period is proportional to the difference between high and low values (Δk as explained earlier in this section). When the stiffness is switched as per control law given in Eq. (4), it results in significant vibration suppression [6].

2.2. Lyapunov-based stability analysis of the switched stiffness method

Theorem 1. *The homogenous version of the quasi time-variant linear system (Eq. (1) with $f(t) = 0$) with the variable-rate stiffness $k(t)$ given by Eq. (4) is globally asymptotically stable in the sense that $y(t) \to 0$ as $t \to \infty$.*

Proof. Choosing the following Lyapunov candidate function:

$$V = \frac{1}{2}\dot{y}^2 + \frac{1}{2}\frac{\bar{K}_1}{m}y^2, \tag{5}$$

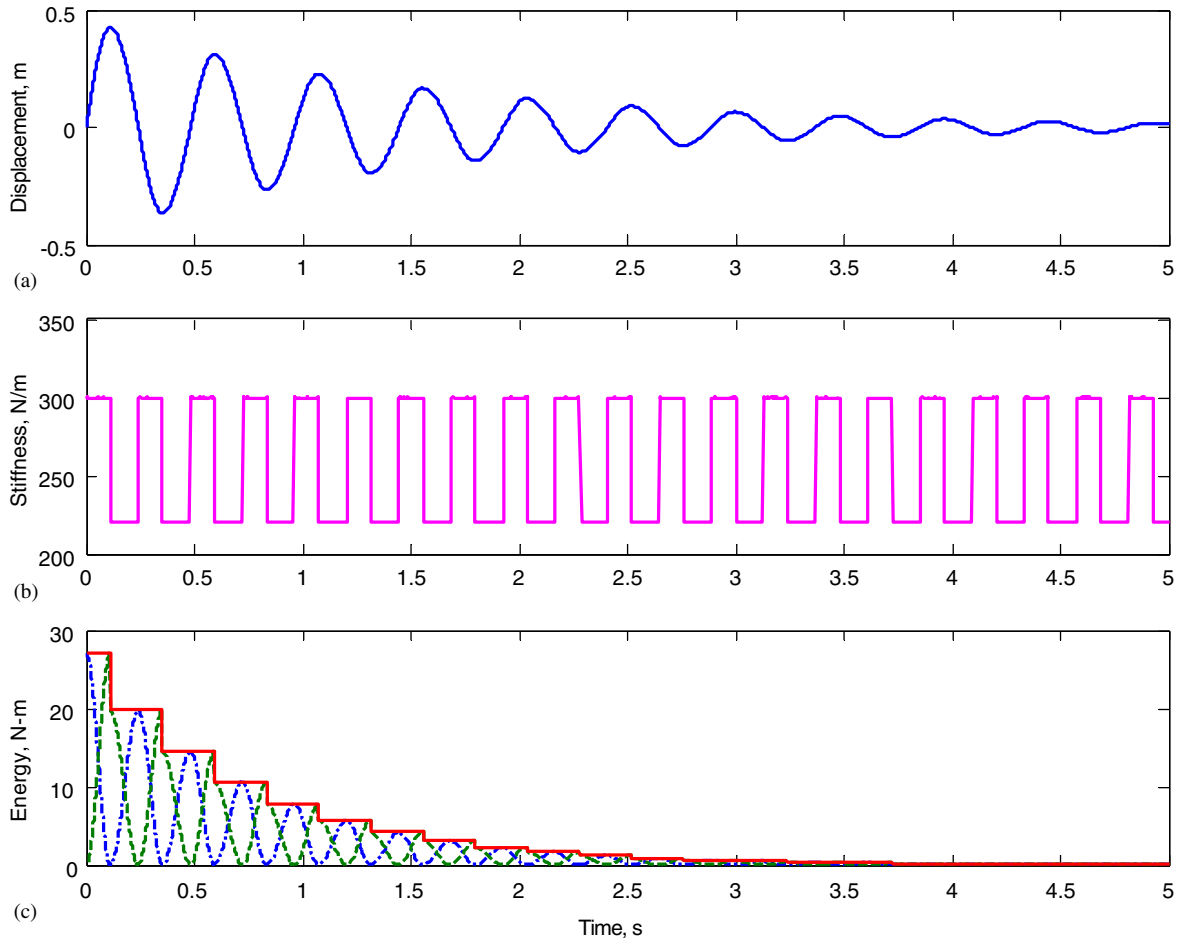

Fig. 2. Illustration of the stiffness switching concept for a sdof system with $m = 1.5\,\text{kg}$, $k_{\text{low}} = 220\,\text{N/m}$ and $k_{\text{high}} = 300\,\text{N/m}$. In (c); dashed–dotted lines (-.-.-.) represent kinetic energy, dashed lines (- - -) represent potential energy, and solid lines (—) represent total energy.

noting its positive definiteness, differentiating it with respect to time and using the homogenous version of Eq. (1), it can be shown that

$$\dot{V} = \left(\ddot{y} + \frac{\bar{K}_1}{m} y\right)\dot{y}. \tag{6}$$

Eq. (6) can be further reduced to

$$\dot{V} = -\frac{\bar{K}_2}{m}|y\dot{y}|. \tag{7}$$

Observing that $\dot{V}$ is negative semi-definite, V is radially unbounded, i.e., $V \to \infty$, as $\|y\| \to \infty$, then, using the Invariant Set Theorem [16], it can be proven that the system given by Eq. (1) with variable spring $k(t)$ is globally asymptotically stable. The phase portrait shown in Fig. 3

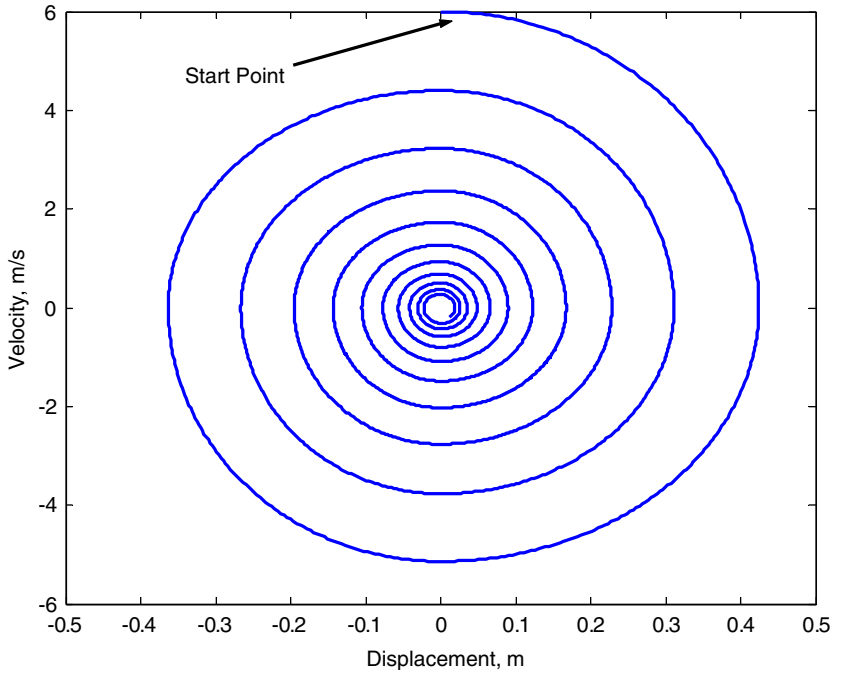

Fig. 3. Phase portrait of the mass–spring system of Fig. 2 with an arbitrary initial velocity indicating system asymptotic stability.

demonstrates this fact which results in a globally asymptotically stable equilibrium point without any limit cycles. □

3. Real time implementation of switched stiffness concept using velocity observer

The control law (4) can be implemented by measuring the position and velocity of the mass–spring system. However, due to the unavailability (or complication of implementation) of velocity sensors, velocity cannot be measured directly, thus hindering the implementation of the control law. In order to overcome this dilemma, a simple solution would be to measure the position and numerically differentiate it to find the required velocity signal. A classical problem associated with this approach is the resulting noise accompanying the differentiated signal leading to erroneous results. To prevent this, a recent robust velocity observer scheme can be utilized to observe the velocity and help implement the control law as developed by Xian et al. [9] and briefly explained next. This observer may also be considered as an inexpensive replacement for the velocity sensors.

3.1. Velocity observer design overview

This section briefly explains the variable structure velocity observer introduced by Xian et al. [9] for a class of unknown nonlinear systems of the form

$$\ddot{y} = h(y, \dot{y}) + G(y, \dot{y})u, \tag{8}$$

where $y(t) \in \Re^n$ is the system output, $u(t) \in \Re^n$ is the control input, $h(y, \dot{y}) \in \Re^n$ and $G(y, \dot{y}) \in \Re^n$ are system nonlinear functions. The following assumptions are made in order to design the observer:

- The system states are always bounded.
- $h(y, \dot{y})$ and $G(y, \dot{y})$ are first order differentiable such that their derivatives exist.
- The control input $u(t)$ is first order differentiable.

If $\dot{\hat{y}}(t)$ is the observed velocity, then the error due to the velocity observation can be given as

$$\dot{\tilde{y}} = \dot{y} - \dot{\hat{y}}. \tag{9}$$

Therefore, to observe velocity accurately, the error should go to zero, i.e., $\dot{\tilde{y}} \to 0$, as $t \to \infty$. In order to achieve this, a second-order filter whose structure is motivated by the Lyapunov-type stability analysis is adopted as follows to generate the needed velocity as

$$\dot{\hat{y}} = p + K_0 \tilde{y}, \tag{10}$$

$$\dot{p} = K_1 \operatorname{sgn}(\tilde{y}) + K_2 \tilde{y}, \tag{11}$$

where $p(t)$ is an auxiliary variable, $\operatorname{sgn}(\cdot)$ denotes the standard signum function, K_0, K_1 and K_2 are positive-definite constant diagonal matrices. The stability analysis using this observer can be performed. However, we prefer not to add additional details here and refer the interested readers to Ref. [9] for more information.

3.2. Modified velocity observer design for switched stiffness

In order to prove the stability of the observer based switched stiffness system, the observer with the structure given in Eqs. (10) and (11) are modified to satisfy the stability criterion as follows:

$$\dot{\hat{y}} = p + K_{01} \tilde{y}, \tag{12}$$

$$\dot{p} = -\frac{2\bar{K}_2}{m} y \operatorname{sgn}(y\dot{\hat{y}}) - \frac{\bar{K}_1}{m} y + K_{02} \tilde{y}, \tag{13}$$

where K_{01} and K_{02} are positive-definite constant diagonal matrices. The stability analysis of this structure is explained in next.

3.3. Lyapunov based stability analysis of switched stiffness method with modified velocity observer

Theorem 2. *The homogenous version of the quasi time-variant linear system (Eq. (1) with $f(t) = 0$) with the variable-rate stiffness $k(t)$ given by control law (4) and velocity observer system (12) and (13) is globally asymptotically stable in the sense that $y(t) \to 0$ as $t \to \infty$.*

Proof. As explained in Section 4, we observe that Eqs. (12) and (13) give the configuration of the observer and can be re-written as

$$\dot{\hat{y}} = p + K_{01} \tilde{y}, \tag{14}$$

$$\dot{p} = V_0 + K_{02}\tilde{y}, \tag{15}$$

where

$$V_0 = -\frac{2\bar{K}_2}{m} y \operatorname{sgn}(y\dot{\hat{y}}) - \frac{\bar{K}_1}{m} y. \tag{16}$$

Differentiating Eq. (14) and with the help of Eq. (15), we get,

$$\ddot{\hat{y}} = V_0 + K_{02}\tilde{y} + K_{01}\dot{\tilde{y}}. \tag{17}$$

Considering $\ddot{\tilde{y}} = \ddot{y} - \ddot{\hat{y}}$ and the homogenous version of Eq. (1), Eq. (17) can be written as

$$\ddot{\tilde{y}} = -\frac{1}{m}k(t) - V_0 - K_{02}\tilde{y} - K_{01}\dot{\tilde{y}}. \tag{18}$$

To prove the stability, we select a Lyapunov candidate as

$$V = \frac{1}{2}\dot{y}^2 + \frac{1}{2}\frac{\bar{K}_1}{m}y^2 + \frac{1}{2}\dot{\tilde{y}}^2 + \frac{1}{2}K_{02}\tilde{y}^2. \tag{19}$$

Differentiating Eq. (19) and substituting Eq. (18) yields,

$$\dot{V} = -\frac{2\bar{K}_2}{m} y\dot{\tilde{y}} \operatorname{sgn}(y\dot{\hat{y}}) - \frac{\bar{K}_2}{m} y\dot{\hat{y}} \operatorname{sgn}(y\dot{\hat{y}}) - K_{01}\dot{\tilde{y}}^2 - \frac{\bar{K}_1}{m} y\dot{\tilde{y}} - V_0\dot{\tilde{y}}, \tag{20}$$

$$\Rightarrow \quad \dot{V} = -\frac{\bar{K}_2}{m} y\dot{\hat{y}} \operatorname{sgn}(y\dot{\hat{y}}) - K_{01}\dot{\tilde{y}}^2. \tag{21}$$

As seen, $\dot{V}(y)$ is negative semi-definite, $V(y)$ is radially unbounded, i.e., $V(y) \to \infty$, as $\|y\| \to \infty$ and

$$\ddot{y} = -\frac{1}{m} y\{\bar{K}_1 + \bar{K}_2 \operatorname{sgn}(y\dot{\hat{y}})\}. \tag{22}$$

Then, using the Invariant Set Theorem [16], it can be proven that system (1) with controller (4) and velocity observer system (12) and (13) is globally asymptotically stable.

4. Simulation result using velocity observer for sdof system

The switched stiffness control concept is implemented using the position and the estimated velocity via the output feedback observer explained earlier. The sdof system in Section 2 is considered with the velocity observer presented in the preceding section for the simulation. Appropriate values for the control gains K_{01} and K_{02} are selected as listed in Table 1. The results for a given initial velocity are obtained as shown in Figs. 4 and 5. The velocity observation error goes to zero (see Fig. 5), as a result of which the observed velocity corresponds to the actual velocity. It must be noted that although the observer does not yield accurate results for some cases, the direction (sign) of the observed signal and the actual signal are in agreement. Such agreement will be more than enough for implementing the switched stiffness control law proposed here. Notice, the control law (4) requires accurate measurement of the velocity signs and not the actual velocity itself.

Table 1
System parameters of the mass–spring system

System parameter	Value	Unit
Mass	1.5	kg
High spring stiffness	300	N/m
Low spring stiffness	220	N/m
K_{01}	2300	—
K_{02}	2500	—

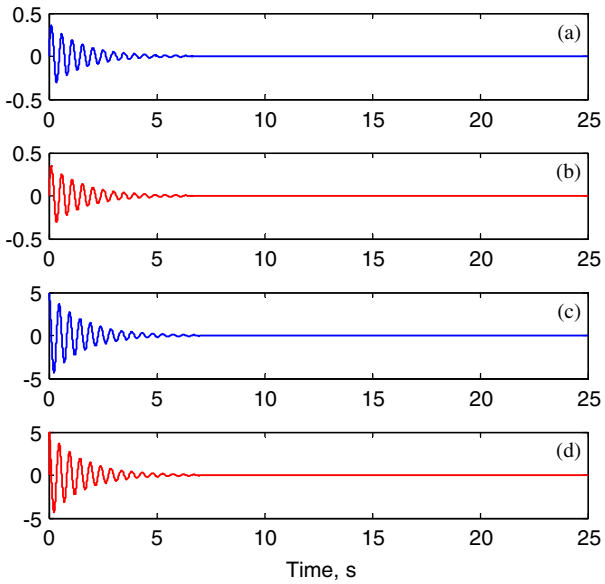

Fig. 4. Velocity observer performance for the switched stiffness method implemented on the sdof system of Fig. 1: (a) position $y(t)$ in [m]; (b) observed position $\hat{y}(t)$ in [m]; (c) velocity $\dot{y}(t)$ in [m/s]; and (d) observed velocity $\dot{\hat{y}}(t)$ in [m/s].

5. Experimental verification of switched stiffness concept

The sdof system with switched stiffness control strategy is considered here for experimental verification. This section presents the experimental setup, implementation of the switched stiffness, and finally experimental results and discussion.

5.1. Experimental setup

A rectilinear plant for multi degree of freedom (mdof) systems is reduced to a sdof system as shown in Fig. 6, [17]. A DC brushless motor excites the mass–spring system. Position feedback is obtained by using an encoder as shown in Fig. 6. The original spring used in the system is modified to take two stiffness values by adding a DC motor controlled arm designed based on a

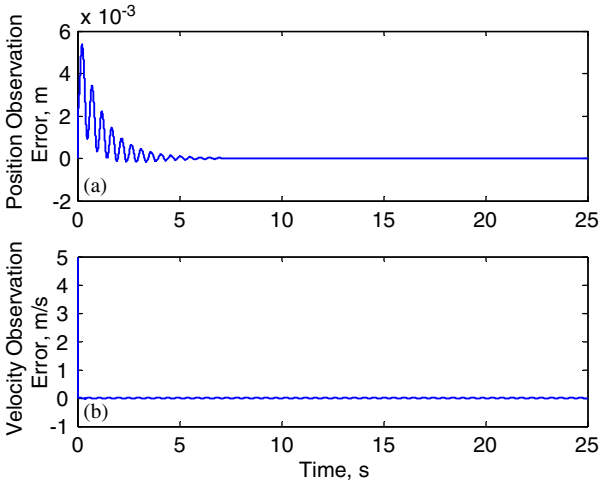

Fig. 5. Position and velocity observation error of the results in Fig. 4.

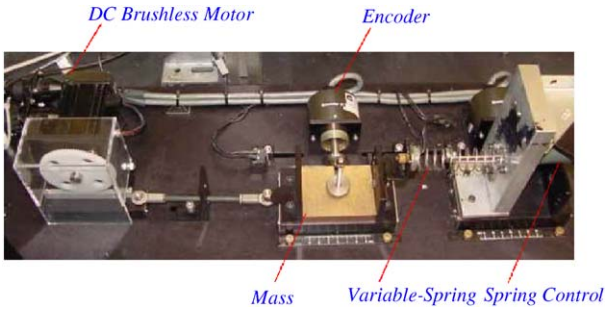

Fig. 6. Experimental setup of the switched stiffness implementation.

similar idea reported by Oda et al. [18]. As shown in Fig. 7, the arm is used to hold the spring at a position making a few active coils inactive, thereby increasing the stiffness (Fig. 7b). The arm is then released to make the spring fully functional, yielding low stiffness configuration (Fig. 7a). Experimental data interfacing is obtained using dSPACE® data acquisition (DS 1104) and controller board. Impulse force is applied to the system using the host computer and an amplifier that drives the DC brushless motor. The experimental setup is shown in Fig. 6, with the experimental parameters the same as numerical simulations listed in Table 1.

5.2. *Arrangement for switching the stiffness*

As explained earlier, one of the practical difficulties in the switched stiffness concept is to have a bi-stiffness spring possessing two stiffness values. Shape memory alloys, electrorheological fluids, magnetorheological fluids, leaf springs and piezoelectric crystals can be used to achieve variable stiffness [10]. However, a simple arrangement extended from an existing design is used here to

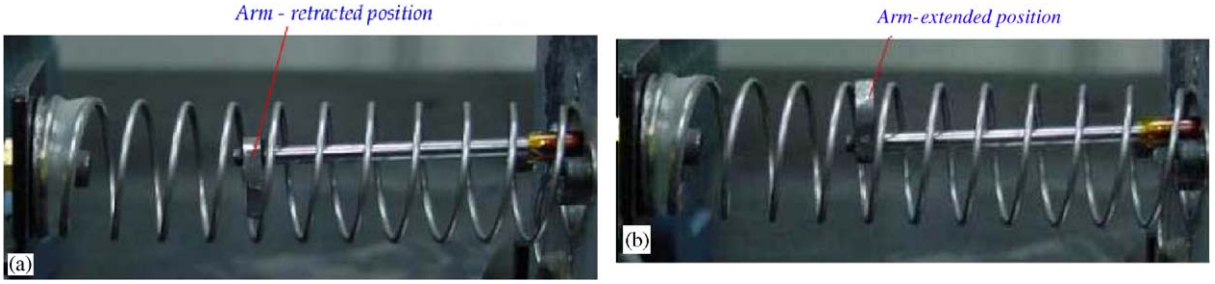

Fig. 7. (a) Low stiffness configuration implementation; (b) high stiffness configuration implementation.

change the stiffness of the spring [18]. The stiffness of a helical spring, which is used in our mass–spring system, depends on the number of active coils present in the spring, which can be represented by the following equation;

$$k = \frac{d^4 G}{8D^3 N}, \tag{23}$$

where d is the diameter of the wire, D is the diameter of the coil spring, N is the number of active spring coils and G is the shear modulus. By changing the number of active coils, the stiffness of the spring can be accordingly changed. By using the external arm design, which runs into the spring, the number of active coils can be changed. The initial design of the arrangement consisted of two arms for effective blocking of coils, but this arrangement resulted in chattering due to lack of synchronization. The effective new design consists of one single arm, which is rotated 180° to block a few active coils corresponding to the high stiffness (Fig. 7b). During low stiffness configuration (Fig. 7a), the arm is retracted inside the spring. The arm extends outside or contracts inside the spring according to the control law with the help of a DC motor and two nylon gears (termed spring control in Fig. 6). Fig. 7 depicts these low stiffness and high stiffness arrangements.

5.3. Experimental results

The experiments were performed for low stiffness, high stiffness and switched stiffness configurations. Fig. 8 depicts the high-level Simulink® block diagram of the switched stiffness implementation wherein position feedback acquisition, velocity signal observation and DC motor controller for the arm are highlighted. The experimental results are shown in Figs. 9 and 10. As seen from Fig. 9, the sdof oscillator response dies out after some time due to the ever-present structural damping in the system. The amplitude of the low stiffness is higher than that of high stiffness.

The switched stiffness is implemented through obtaining position feedback using the encoder, estimating the velocity using the variable structure observer and implementing the control law (given by Eq. 4). The control law gives an output signal that will activate the DC motor to operate the arm in order to switch the stiffness. The switched stiffness results in less settling time as expected (see solid lines in Fig. 9). The results shown in Figs. 9 and 10 are obtained using the velocity observer to estimate the velocity. The bottom graph of Fig. 10 shows the control action to

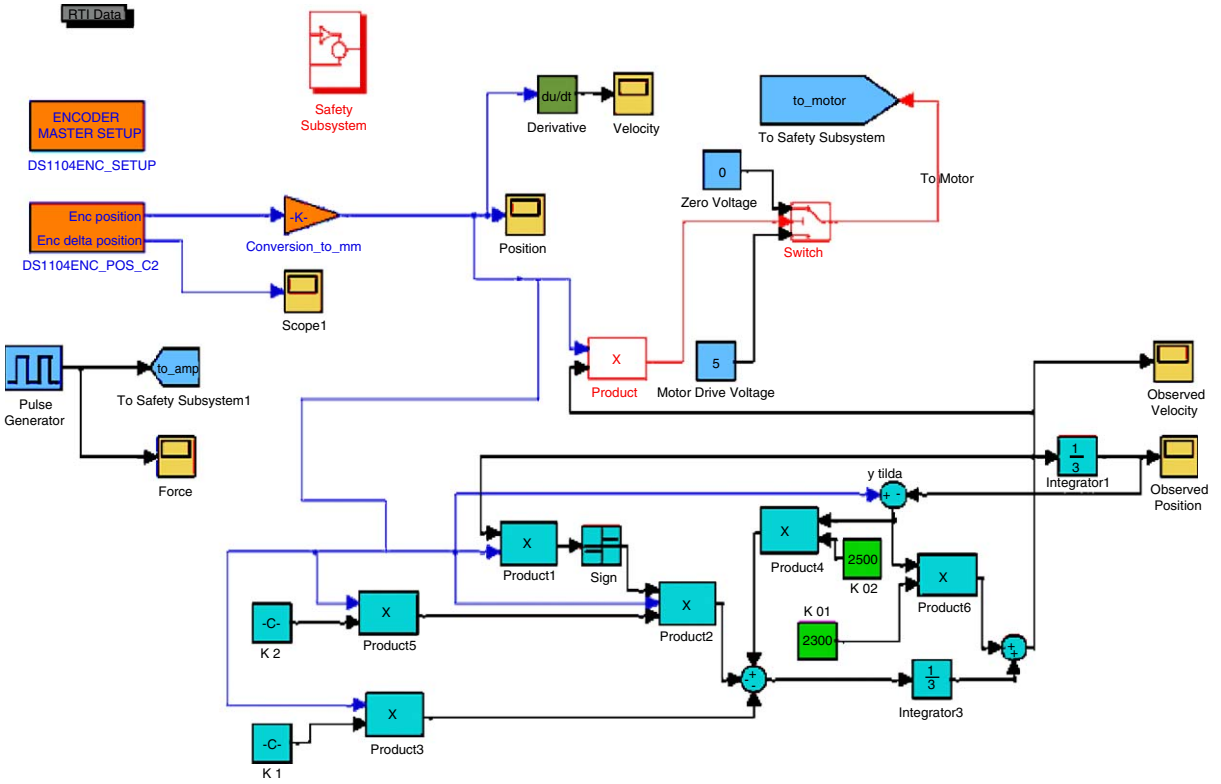

Fig. 8. High-level Simulink block diagram of the position feedback and velocity observer.

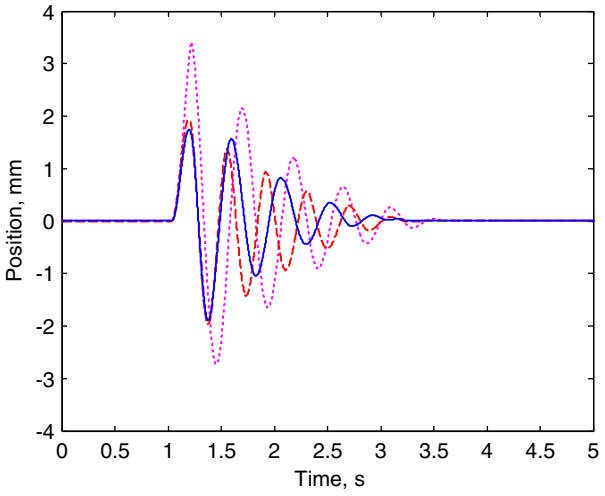

Fig. 9. Experimental response of the sdof system for different stiffness values; dotted lines (…..) represent low stiffness, dashed lines (- - - -) represent high stiffness, and solid lines (—) represent switched stiffness.

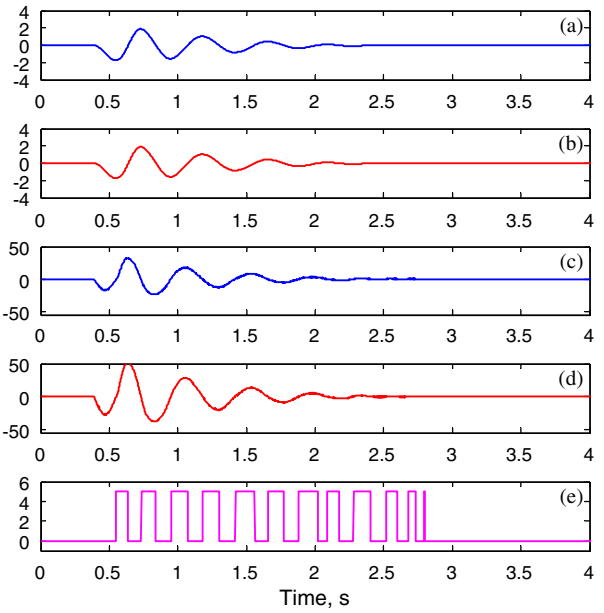

Fig. 10. Experimental implementation results using velocity observer: (a) position $y(t)$ in [mm]; (b) observed position $\hat{y}(t)$ in [mm]; (c) velocity $\dot{y}(t)$ in [mm/s]; (d) observed velocity $\hat{\dot{y}}(t)$ in [mm/s]; and (e) switching control in [V].

switch the stiffness. This control action operates a relay, which switches the DC motor to change the arm's position (the DC motor cannot be directly operated by the computer due to output current limitations).

In order to better compare the controlled system with uncontrolled case (either low or high stiffness), the area under the curve in Fig. 9 and their corresponding plots are shown in Fig. 11. It is noted that the switched stiffness has less "error area" than the low stiffness and high stiffness curves (area of **1147** compared to low stiffness of **2066** and high stiffness of **1263**). The high stiffness results seem closer to the switched stiffness because of the time delay and ineffective switching mechanism. However, the simulation results of the system when utilizing experimental parameters (damping assumed to be viscous for simplicity) yield better results for the switched stiffness case as shown in Fig. 12. The main reason for the existence of a disparity between these numerical results (Fig. 12) and experimental results of Fig. 9 is due to the experimentally calculated equivalent viscous damping coefficients for the low stiffness and high stiffness settings. This is due to extra dynamics that come into picture by adding an external arm in the spring to simulate high stiffness. Just for consistency in the reported results, one of the damping coefficients has been chosen for simulation of all the three cases (high stiffness, low stiffness and switched stiffness). Moreover, the impulse used in the simulations and the impulse used in the experiment may not produce the same results or cannot be implemented similarly due to the actuator limitation. It must also be noted that our intention for providing simulation results using experimental parameters is not to compare the experimental results with the simulations. Instead, this plot (Fig. 12) is provided to prove that the switched stiffness concept can be used more

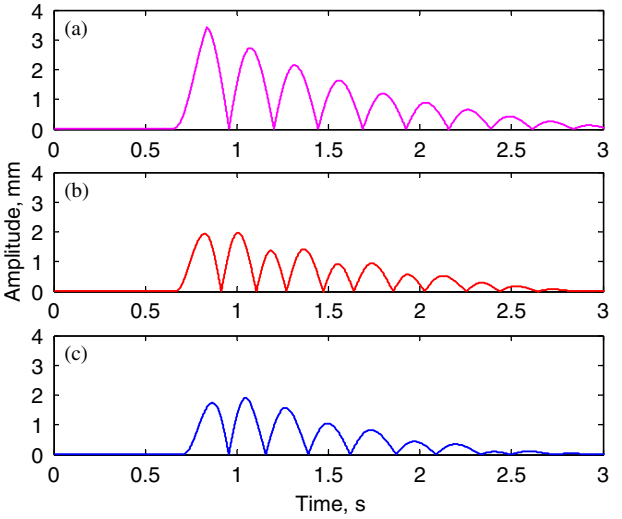

Fig. 11. The "error area" under the response curve ($y(t)$) for different stiffness configurations: (a) low stiffness with area of **2066**; (b) high stiffness with area of **1263**; and (c) switched stiffness with area of **1147**.

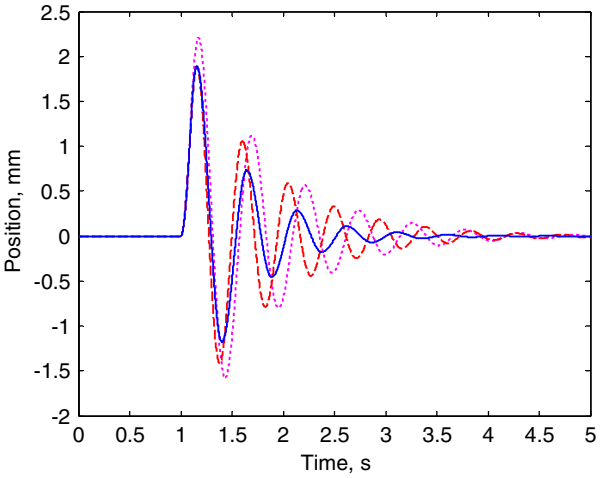

Fig. 12. Simulation results of system output ($y(t)$) when utilizing experimental system parameters; dotted lines (…..) represent low stiffness, dashed lines (- - - -) represent high stiffness, and solid lines (—) represent switched stiffness.

effectively to suppress vibrations (i.e., as another case of numerical simulation with damping in the system).

The FFT of the experimental responses is shown in Fig. 13, where the lower amplitude ratio of the switched stiffness configuration (when compared to low and high stiffness cases) is to be noted. The switched stiffness experimental results using numerical differentiation for the velocity signal requirement is also shown in Fig. 14. It is seen that, both the numerical differentiation and

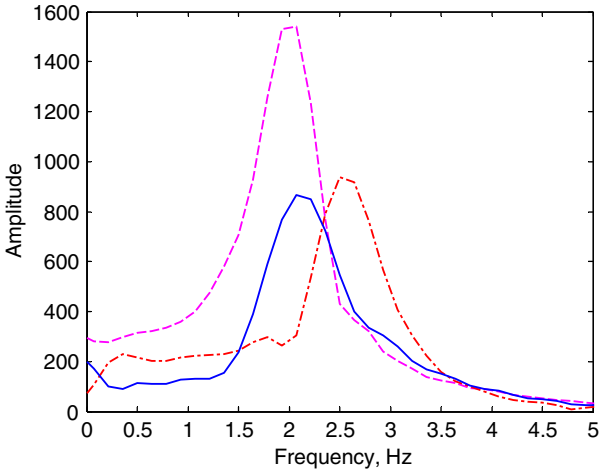

Fig. 13. Experimental frequency domain response of the system (FFT$\{y(t)\}$) for different stiffness values; dashed lines (- - - -) represent low stiffness, dashed–dotted lines (-.-.-.-) represent high stiffness, and solid lines (—) represent switched stiffness.

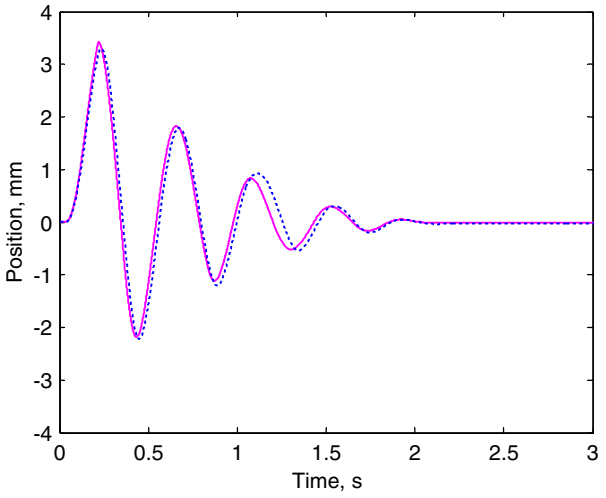

Fig. 14. Comparison of switched stiffness method when using velocity observer and numerical differentiation for system output $y(t)$; solid lines (—) represent observer results, dotted lines (…..) represent results obtained using numerical differentiation.

the observer give similar results. However, this may not be the general case when position feedback is given through other types of position sensors such as laser displacement sensors (the noise levels are much higher compared to optical encoders). Thus, the simulation and experimental results indicate green lights for implementing the switched stiffness control concept for effective suppression of vibrations.

6. Conclusions

The concept of switched stiffness was explained using a simple sdof system. Through switching the stiffness, depending on the position of the system with respect to the equilibrium state, energy dissipation was maximized and considerable vibration suppression was achieved. Real-time implementation difficulty with regard to velocity measurement was overcome using an output feedback variable structure observer. Experimental validation of the vibration attenuation using switched stiffness technique with the velocity observer was also demonstrated. These results provided here could pave the way for semi-active vibration control of systems using piezoelectric materials, which can easily change their stiffness according to the type of circuit connection.

Acknowledgement

The authors would like to thank Prof. Darren Dawson from Clemson University, Department of Electrical and Computer Engineering, for his help on velocity observer design and stability proof analysis.

References

[1] M. Dadfarnia, N. Jalili, B. Xian, D.M. Dawson, A Lyapunov-based piezoelectric controller for flexible cartesian robot manipulators, *ASME Journal of Dynamic Systems, Measurements and Control* 126 (2) (2004) 347–358.
[2] N.W. Hagood, A. Von Flotow, Damping of structural vibrations with piezoelectric materials and passive electrical networks, *Journal of Sound and Vibration* 146 (2) (1991) 243–268.
[3] N. Jalili, A new perspective for semi-automated structural vibration control, *Journal of Sound and Vibration* 238 (3) (2000) 481–494.
[4] N. Jalili, A comparative study and analysis of semi-active vibration-control systems, *ASME Journal of Vibration and Acoustics* 124 (2002) 593–605.
[5] W.W. Clark, Vibration control with state-switched piezoelectric materials, *Journal of Intelligent Material Systems and Structures* 11 (4) (2000) 263–271.
[6] A. Ramaratnam, N. Jalili, D.M. Dawson, Semi-active vibration control using piezoelectric-based switched stiffness, *Proceedings of American Control Conference*, Boston, MA, 2004.
[7] A. Ramaratnam, N. Jalili, M. Grier, Piezoelectric vibration suppression of translational flexible beams using switched stiffness, *Proceedings of 2003 International Mechanical Engineering Congress and Exposition* (IMECE 2003-41217), Washington DC, 2003.
[8] A. Ramaratnam, Semi-active vibration control using piezoelectric-based switched stiffness, Master's Thesis, Department of Mechanical Engineering, Clemson University, 2004.
[9] B. Xian, M.S. de Queiroz, D.M. Dawson, M.L. McIntyre, Output feedback variable structure control of nonlinear mechanical systems, *Proceedings of IEEE Conference on Decision and Control*, Hawaii, 2003.
[10] P.L. Walsh, J.S. Lamancusa, A variable stiffness vibration absorber for minimization of transient vibrations, *Journal of Sound and Vibration* 158 (1992) 195–211.
[11] D.C. Nemir, Y. Lin, R.A. Osegueda, Semiactive motion control using variable stiffness, *Journal of Structural Engineering* 120 (4) (1994) 1291–1305.
[12] M.A. Franchek, M.W. Ryan, R.J. Bernhard, Adaptive passive vibration control, *Journal of Sound and Vibration* 189 (5) (1995) 565–585.
[13] L.R. Corr, W.W. Clark, Energy dissipation analysis of piezoceramic semi-active vibration control, *Journal of Intelligent Materials Systems and Structures* 12 (2001) 729–736.

[14] C. Richard, D. Guyomar, D. Audigier, G. Ching, Semi-passive damping using continuous switching of a piezoelectric device, *Smart Structures and Materials, Passive Damping and Isolation* 3672 (1999) 104–111.
[15] L. Meirovitch, *Fundamentals of Vibrations*, McGraw Hill, New York, 2001.
[16] J.J. Slotine, W. Li, *Applied Nonlinear Control*, Prentice-Hall, Englewood Cliffs, NJ, 1991.
[17] http://www.ecpsystems.com/dynamics_recplant.htm (last accessed on May 1, 2004).
[18] J. Oda, A. Wang, N. Matsumoto, Trial formation of variable-stiffness spring and its application to displacement control problems, *Transactions of Japan Society of Mechanical Engineers, Series C* 59 (564) (1993) 2526–2531.